Case Studies in Thermal Engineering 53 (2024) 103742

Contents lists available at ScienceDirect

Case Studies in Thermal Engineering

journal homepage: www.elsevier.com/locate/csite

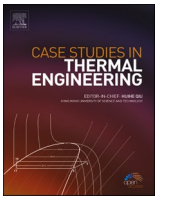

Experimental investigation on acceleration of working fluid of heat pipe under bypass line operation

Cheong Hoon Kwon [a], Hyuk Su Kwon [b], Hyun Ung Oh [c,**], Eui Guk Jung [b,*]

[a] School of Mechanical System Engineering, Kangwon National University, Kangwon-do, 25913, Republic of Korea
[b] Department of Energy Resources and Chemical Engineering, Kangwon National University, Kangwon-do, 25913, Republic of Korea
[c] Department of Aerospace Engineering, Korea Aerospace University, Gyeonggi-do, 10540, Republic of Korea

ARTICLE INFO

Keywords:
Heat pipe
Liquid bypass line
Thermal resistance
Thermal performance
Flow resistance
Working fluid acceleration

ABSTRACT

In a conventional heat pipe, the flow resistance is generated by the opposing flow of liquid and vapor across the phase-change interface. The flow resistance can impose a limitation on the heat transfer rate within the heat pipe, which can have an adverse effect on its overall efficiency. Therefore, reducing the flow resistance is essential for improving the heat transfer of heat pipe. The method of inducing a decrease in flow resistance is classified as an essential technology for improving the heat transfer performance of a heat pipe. In this study, experiments were conducted to induce operating fluid acceleration by decreasing the hydrodynamic resistance inside a heat pipe to improve thermal performance. A liquid bypass line connecting the three points of the condenser to the beginning of the evaporator was designed and installed, with four flow rate control valves attached to control the bypass flow rate at each bypass port. In this study, the working fluid acceleration was observed experimentally in bypass mode (all bypass valves opened) and normal mode (all bypass valves closed). According to the experimental results, the heat transfer efficiency of the heat pipe system improved by up to 106.5% in relation to the thermal resistance. The maximum thermal load in a horizontal position increased by up to 45.8% in the bypass mode.

Nomenclature

BM	bypass mode
BL	bypass line
BLFV	bypass line flow valve
NM	normal mode
Q	thermal load (W)
T	temperature (°C)
$\overline{T}$	mean temperature (°C)
U	uncertainty
φ	inclination angle of the heat pipe (degree)
Φ	fill–charge ratio of working fluid

* Corresponding author.
** Corresponding author.
E-mail addresses: chkwon2@kangwon.ac.kr (C.H. Kwon), ohu129@kau.ac.kr (H.U. Oh), egjung@kangwon.ac.kr (E.G. Jung).

https://doi.org/10.1016/j.csite.2023.103742
Received 20 June 2023; Received in revised form 20 October 2023; Accepted 7 November 2023
Available online 29 November 2023

Subscripts

adia	adiabatic
BL	bypass line
con.	condenser
cool. in	coolant inlet
cool. out	coolant outlet
eva.	evaporator
in	input
max.	maximum value
m	measurement

1. Introduction

1.1. Literature review

The principle of the typical heat pipe originated from the "Heat Transfer Device" patented in 1942 by Gaugler [1] of GM in the United States. The term "heat pipe" was first used for the "Evaporation-Condensation Heat Transfer Device" patented by Grover [2] of the Los Alamos Laboratory in the United States in 1963. Today, typical heat pipes are used in a variety of cooling applications, such as those for airplanes, medical devices, power electronics cooling, and space technologies.

As shown in Fig. 1, a typical heat pipe has a cylindrical cross section with a capillary structure installed in close contact with the inner wall, and a working fluid is filled inside the heat pipe with a high vacuum. Inside a typical heat pipe, the counter flow of liquid and vapor results in flow resistance at the interface between the two phases, as depicted in Fig. 1. The influence of gravity on the inclination angle can cause a significant change in the performance of the typical heat pipe by affecting the flow resistance. Even with the use of capillary pressure the return of the liquid under the influence of gravity becomes impossible under operating conditions where the evaporator is located above the condenser. Although these limitations exist in the operation of typical heat pipes, as shown in Fig. 1, the typical heat pipes exhibit excellent heat transfer performance, including high effective thermal conductivity, passive operation, and isothermal operation. Because typical heat pipes have no moving parts and a simple structure, they are easy to manufacture and maintain, and they are widely used because they have a long service life.

The operation of a typical heat pipe has several limitations [3] such as the capillary limit, which causes dryout. The capillary limit is easily observed in typical heat pipe experiments because it occurs at the lowest temperature. To observe other operating limits, appropriate experimental conditions and restricted operating conditions may be required. Capillary pressure is the key driving force behind the operation of the heat pipe, and selecting the right capillary structure design or working fluid can enhance heat transfer performance of the heat pipe. Thus, investigations aiming to lower the thermal resistance through decreasing the operating temperature while maintaining a constant input thermal load to enhance the heat transfer capability of a heat pipe have predominantly centered on optimizing the wick design or selecting the appropriate working fluid. In research focusing on the design of capillary wicks, Zhao et al. [4] applied a novel sintered multisize copper powder wick (SMW) as a flat micro-heat pipe wick structure. This SMW reduced the liquid movement time by 16.59% compared with that of screen mesh wicks. The overall heat transfer resistance was lowered by 14.22%. Zhao et al. [5] experimented with a sodium heat pipe that used screen wire wicks with different mesh numbers and showed that an intense-pore/scarce -pore/intense-pore screen synthesis had enhanced heat transfer performance than other screen wick combinations. Ginting et al. [6] fabricated a wick structure with completely new stainless-steel foam and applied it to a cylindrical heat pipe, which was tested horizontally; however, the heat transfer performance compared with other capillary structures was not reported. Jiang et al. [7] fabricated a heat pipe with wicks of three different pore sizes to enhance the heat transfer efficiency under conditions of anti-gravity orientations. In their experiment, the use of a hybrid wick, which combined a coarse powder and a nanoporous fine powder, resulted in a significant improvement in heat transfer performance when the system was subjected to an anti-gravity orientation. Wong and Liao [8] fabricated a heat pipe incorporating a wick made of sintered composite copper mesh grooves and investigated its heat transfer capability. They visually presented the drying phenomenon in the wick structure and demonstrated improved heat transfer compared to other screen mesh wicks when the composite wick was used. Cui et al. [9] fabricated an ultrathin, flat heat pipe to control the heat of a high-power electronic device. They applied a screen wire mesh wick oxidized using thermal oxidation to improve the capillary force by increasing the hydrophilicity of the wick casting and obtained a relatively low thermal resistance under conditions wherein the electronic device could operate stably. Huang et al. [10] fabricated a novel composite

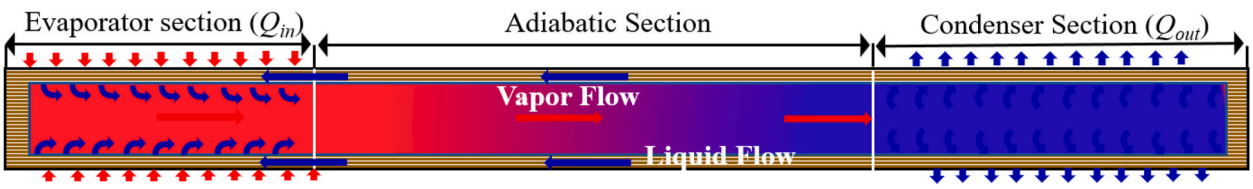

Fig. 1. Schematic of a typical heat pipe showing circulation of working fluid.

wick made of stainless-steel fibers and powder to improve the driving force and developed a capillary structure with excellent permeability. Applying the new wick resulted in improved heat transfer performance, and the increase in performance was 2.64 times the value of a conventional wick.

Many studies have been conducted for selecting a working fluid to improve the heat pipe performance. Henein and Abdel-Rehim [11] conducted an experimental study on a heat pipe for solar collectors that used a new hybrid nanofluid composed of magnesium oxide (MgO) and multi-walled carbon nanotubes (MWCNTs) as an operating fluid. They obtained the highest heat collection efficiency by using equal proportions of MgO and MWCNT. Zhang et al. [12] fabricated a flat-plate heat pipe and compared its heat transfer performance by applying a water-based nanofluid with Al_2O_3 particles and other pure working fluids. Application of the nanofluid resulted in a reduction in thermal resistance of up to 58.7% as compared to other working fluids. The thermal performance of a heat pipe using a nanofluid containing dolomite particles in ethylene glycol was investigated by Ref. [13], and the heat transfer performance was improved by up to 65% by applying nanofluid with dolomite/ethylene glycol as the working fluid. The heat transfer performance of a thermosyphon using bauxite nanofluid and an anionic surfactant was measured by Aydın et al. [14], and the thermal resistance was found to be lowered by up to 24.3%. In addition, a study [15] confirmed the remarkable superiority of thermal performance of heat pipes using deionized water/bauxite nanofluid as a working fluid among various nanofluids. In experiments on the thermal performances of heat pipe heat exchangers using nanofluid as the working fluid [16,17], the thermal efficiency of a heat exchanger with a hybrid nanofluid mixed with two types of nanoparticles was improved by up to 63%. Additionally, that of a heat pipe heat exchanger using magnetic nanofluids [17] as the working fluid was improved up to 87.2%. Zhang et al. [18] adopted a magnetic fluid, which could flow under the influence of a magnetic field, as the operational fluid in a heat pipe for the thermal management of electronic devices. They obtained a heat transfer performance equivalent to that of water. As a working fluid in a heat pipe for solar collectors, Jahanbakhsh et al. [19] used a blend of ethanol and water mixed in a certain proportion to prevent freezing during winter. They found that an optimal mixing ratio resulted in the highest heat transfer performance.

Meanwhile, the heat transfer performance has been improved by structurally changing heat pipes in consideration of physical considerations of working fluid flow. In typical heat pipe operation, heat transfer is known to be significantly limited due to flow resistance over the interface caused by counter flows of vapor and liquid inside the heat pipe [20]. To fundamentally overcome these limitations, heat pipes with a loop form in which vapor and liquid are completely separated have been widely developed [21]. Wu et al. [22] manufactured a new type of heat pipe in which the evaporator and condenser were completely separated through vapor and liquid tubes to be suitable for cooling the spent fuel pool cooling system, and the cooling performance of the designed device was experimentally investigated. The heat transfer performance of a loop-type pulsating heat pipe was experimentally investigated by Kang et al. [23]. Their model predicted a significant improvement in heat transfer performance by installing a porous wicking layer [24] and separating walls inside the flow channel [25]. Furthermore, they fabricated a flexible transport tube for vapor and liquid and a pulsating heat pipe with multiple heat sinks, and the thermal performance of the designed device was experimentally investigated. In particular, considerable flexibility in spatial arrangement can be guaranteed by a system with flexible transport tubes for vapor and liquid. In addition, the application of multiple condensers was evaluated as a technology that allows simultaneous thermal control by combining multiple electronic components into one module.

Heat pipes in which vapor and liquid are completely separated clearly have significantly improved heat transfer performance compared to that of typical heat pipes because the flow resistance caused by the counter flow of vapor and liquid can be fundamentally eliminated. In particular, such heat pipes are known to have the outstanding advantage of being able to operate normally in an operating environment without gravity assistance, where the evaporation unit is located above the condenser [20]. However, a fairly high level of technology is required in the design and manufacture of heat pipes with loop types. In particular, to ensure the unique and excellent performance of a typical loop heat pipe, a high-level sintering technology that must meet fairly precise standards in porosity, pore size, and permeability for fine porous wick is essential. Because of this, there are high economic limitations in the application of thermal control to terrestrial electronic equipment that requires mass production under fairly high manufacturing costs. Due to manufacturing difficulties and high design/manufacturing costs, typical loop heat pipes have been designed and manufactured in some spacecraft developing countries and applied only to space vehicle thermal control [26–28].

1.2. Heat pipe with liquid bypass line

In relatively recent studies [29–32], experiments were conducted to improve the heat transfer performance by reducing flow resistance caused by counter flows of vapor and liquid through consideration of the flow of working fluid inside a typical heat pipe. Flow resistance over the phase change interface between vapor and liquid with counter flow inevitably occurs inside the heat pipe. Because of this, the performance is inevitably deteriorated and accompanied by a pressure drop in the working fluid. In their studies [29,30], a bypass line was designed so that some of the liquid inside the condenser could be bypassed to the evaporator without passing through the heat pipe. The maximum input thermal load [29] of the heat pipe with the application of the bypass line was improved by up to 35.5%, and the thermal resistance [30] was reduced by up to 61% under steady-state operation. Furthermore, tendencies in the thermal behavior of heat pipes with increasing mass flow rate into the bypass tube were investigated by Cheong et al. [31,32]. Especially, in their study, three bypass ports were installed in the condenser to increase the condenser area open to the bypass tube. The maximum input thermal load and thermal resistance under steady-state conditions according to the number of activated bypass ports were experimentally investigated. When all three bypass ports were opened, the maximum input heat load [31] and heat transfer performance under steady-state operation [32] increased by up to 45.8% and 59.4%, respectively, compared to those of a typical heat pipe.

As presented in the literature [29–32], a heat pipe with a bypass line differs from a loop heat pipe with complete separation of vapor and liquid in that the vapor and liquid are partially separated. Therefore, a heat pipe with a bypass line partially takes advantage of the

loop-type heat pipe and is much simpler and economical in manufacturing and design. Previous studies [29–32] have shown that liquid bypass can contribute to improving the heat transfer performance of heat pipes, and that the thermal performance can be improved with a more appropriate design of the bypass tube. As shown in Figs. 2 and 3(b), the liquid in the condenser can be partially separated by the bypass line. Liquid can be bypassed with a bypass line located below the heat pipe, and vapor with that located above the heat pipe. In particular, the theoretical background and principles for improving the heat transfer performance of heat pipes under bypass operation were provided in detail in the literature [29,31]. As suggested, as the amount of liquid or vapor being bypassed increases, the flow resistance in the internal space of the heat pipe decreases, thereby inducing acceleration of the working fluid, which can be expected to improve heat transfer performance. Therefore, the bypass line should be designed so that as much working fluid as possible can be bypassed.

This study was conducted as an extension of previous studies [29–32]. Previous studies have not presented experimental results on the acceleration of the working fluid under bypass line operation. Although the background and principles for improving heat transfer in heat pipes by liquid bypass have been theoretically provided in the literature [31,32], experimental results on acceleration of the working fluid with reduced flow resistance inside the heat pipe have not been provided. Therefore, the purpose of this study was to experimentally observe the phenomenon of acceleration of the working fluid under the operation of the bypass line. There is currently no known method for measuring pressure and flow rate by measurement because heat pipes operate under saturated conditions with two-phase flow. In general experiments, the behavior of the working fluid has been described by the temperature distribution on the heat pipe wall. Therefore, the acceleration of the working fluid can be explained by the temperature distribution on the condenser wall. In this study, the acceleration of the working fluid was evaluated by the temperature measured by three thermocouples attached to the condenser. The more the working fluid is accelerated, the more vapor reaches the end of the condenser. This can result in an increase in the temperatures measured by a thermocouple attached to the surface of the condenser. Therefore, the experiment was performed under the assumption that higher temperatures measured by a thermocouple attached to the condenser wall would greatly accelerate the vapor. In particular, to maintain consistency with the experiments of previous studies, the geometric size and shape of the heat pipe with the liquid bypass tube installed are the same as those in literature [31,32].

In bypass mode (*BM*) (all bypass valves activated) and normal mode (*NM*) (all bypass valves closed), the working fluid acceleration was experimentally described using the temperature distribution in the heat pipe. The heat pipe was started in the *NM* and switched to the *BM* after achieving a steady-state operation to accomplish the goal of this experimental study. The acceleration performance of the working fluid was examined by comparing the condenser wall temperatures in *NM* and *BM*.

2. Experimental setup and procedure

An experimental device was constructed to observe the acceleration capability of a working fluid in a heat pipe through a liquid bypass implemented by means of a bypass line. Fig. 3(b) depicts an image of the heat pipe containing the bypass tube fabricated in this research. The geometric size and capillary structure of the basic heat pipe were identical to those used in previous studies [31,32], with three bypass ports installed in the condenser. As shown in Fig. 3(b), bypass ports were attached to the beginning, middle, and end of the condenser at regular intervals. A bypass port was installed at the beginning of the evaporator. A bypass line was designed to connect these ports, with an on/off valve installed at each port to control activation or deactivation of the bypass line, as illustrated in Fig. 3(b). The heat pipe and bypass tube are made of aluminum. As depicted in Fig. 4, the distance between the internal and external surfaces of the wall was 1 mm, while the outer and inner diameters were 15.88 mm and 13.88 mm, respectively. Grooves were produced on the inside wall of the heat pipe to supply the capillary pressure required for the working fluid circulation, as shown in Fig. 4. In particular, trapezoidal grooves supply the driving force required for the circulation of the working fluid. The grooves measured 2 mm in height, with a bottom length of 0.7 mm and a tip length of 0.93 mm. Considering the compatibility between the tube made of aluminum and the working fluid, acetone with 99% purity was used as the working fluid. The internal space of the heat pipe was filled under a maximum pressure of 1×10^{-5} torr by an oil diffusion pump capable of providing high vacuum. Out of the overall length of 750 mm, the evaporator and condenser measured 200 mm in length each, while the adiabatic section measured 350 mm in length. The liquid bypass line, consisting of a plain tube with an outer diameter of 6.35 mm, was connected to ports attached at the beginning, middle, and terminal point of the condenser. Figs. 2 and 3 shows that the position and number of ports installed in the condenser significantly affect the rate of liquid flowing through the bypass line.

As shown in Fig. 5, 30 AWG thermocouples, which had a wire diameter of 0.25 mm were installed along the longitudinal direction of the heat pipe to determine an estimation of the temperatures at seven important locations. The thermocouples used to obtain the

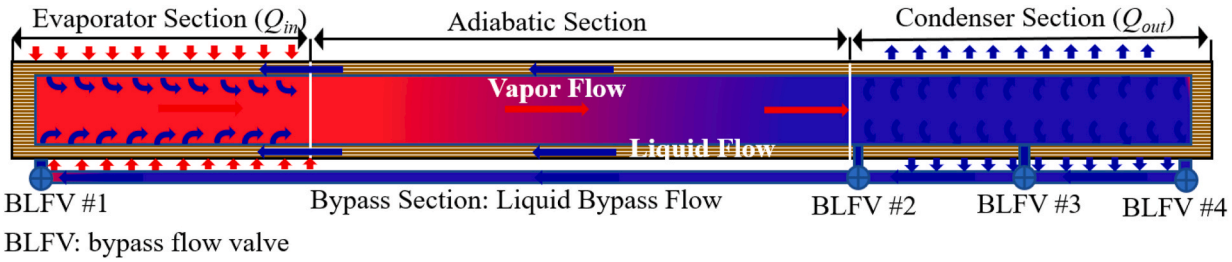

Fig. 2. Schematic of the physical operation of a heat pipe with a liquid bypass tube.

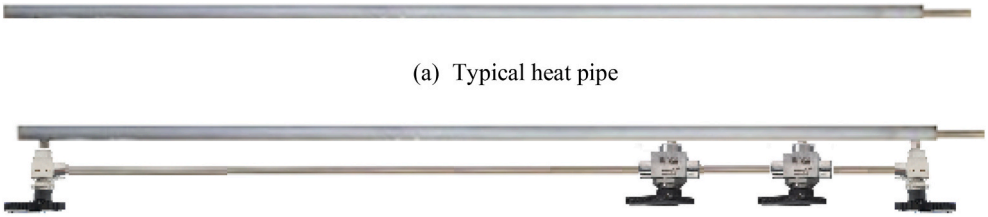

(a) Typical heat pipe

(b) Typical heat pipe with three bypass ports in the condenser

Fig. 3. Photographs of a typical heat pipe and a heat pipe with a bypass line [31,32].

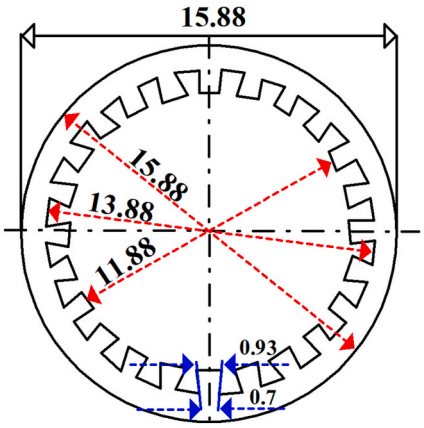

Fig. 4. Cross-sectional dimensions of a heat pipe with grooves.

evaporator wall temperatures ($T_{eva.1}$, $T_{eva.2}$, and $T_{eva.3}$) were attached at the beginning, middle, and end of the evaporator at 100 mm intervals. The thermocouples used to measure the condenser temperatures ($T_{con.1}$, $T_{con.2}$, and $T_{con.3}$) were attached at 98 mm intervals. A thermocouple, which was fixed to the center of the heat pipe, was used to obtain the temperatures in the adiabatic section ($T_{a.}$). Typically, in heat pipe experiments, the temperature of the adiabatic section can be defined as the operating temperature, liquid temperature, and vapor temperature under local equilibrium between liquid and vapor. The liquid bypass flow was detected using four thermocouples (T_{BL1}, T_{BL2}, T_{BL3}, and T_{BL4}) positioned on the wall of the liquid bypass tube. The thermocouples were attached to the valve outlets to detect the liquid flow at each bypass port. Thermocouples of the probe type, having outer diameters of 3 mm, were employed to measure the temperatures ($T_{cool.in}$ and $T_{cool.out}$) at the entrance and exit of the cooling jacket that enveloped the condenser. The recovered heat discharged from the heat pipe into the coolant was evaluated using the entrance and exit temperatures of the heat sink jacket. The calibration process for these thermocouples was carried out with an error margin of 0.1 °C or less using a standard thermometer in a specified temperature range (5–100 °C). Water was used as the coolant in the experimental device and was consistently maintained temperature with the aid of an isothermal circulating bath. An isothermal bath with a constant temperature capacity of up to 1 kW at 3 °C was adopted. A constant volumetric flow rate of 3 L/min remained for the coolant during the entire experiment. The maximum uncertainty of the rotameter used to measure the flow rate was 4 L/min at full-scale. A voltage regulator was utilized to maintain a constant thermal load on the heat pipe system. The input thermal power was determined by means of a wattmeter with a maximum uncertainty of 0.5% of the full scale. A Q_{in} to the heat pipe was supplied by four 1-kW cartridge heaters inserted into a heater block that enveloped the entire evaporator. Considering that the maximum input thermal load that a heat pipe can tolerate can be significantly increased depending on the orientation of the heat pipe, type of working fluid, and cooling conditions, the capacity of the heater was selected to ensure that a sufficient thermal load can be supplied. The measurement instrument uncertainties used in the heat pipe experimental setup are provided in Table 1.

These uncertainties were provided by a professional calibration company for the instrument. The uncertainty of the measuring device can be evaluated as described in Refs. [32–34], and that of the experimental setup with N instruments can be expressed as follows using the square root of the sum of the squares:

$$U_m = \sqrt{U_1^2 + U_2^2 + U_3^2 + \ldots + U_N^2} \tag{1}$$

When the uncertainty of each of the five instruments presented in Table 1 was calculated according to Eq. (1), the uncertainty of the experimental setup was evaluated to be 4%. All the temperature data were monitored and stored every second through the use of a data acquisition system. To prevent the production of non-condensable gas inside the heat pipe all components of the heat pipe were cleaned with acetone (a cleaning agent) using an ultrasonic cleaner. The experimental procedure was conducted in a laboratory setting

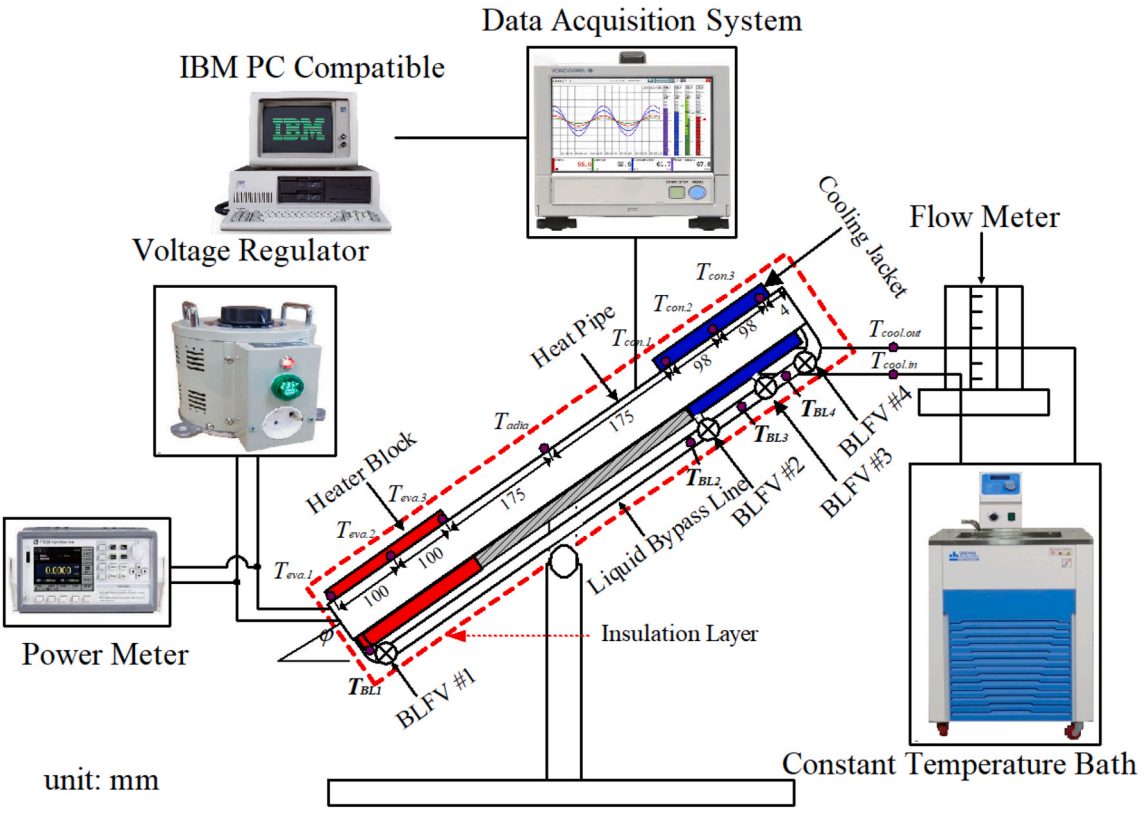

Fig. 5. Experimental setup of the heat pipe system, including the thermocouple locations considered in this work.

Table 1
Uncertainties of the instruments used in experiments [32].

Independent variable	Error (gauge)	Uncertainty
Thermocouple (OMEGA, K-type, 30 AWG)	0.5 °C	0.00175
Thermal load (ITECH, IT9121)	0.5%	0.005
Isothermal bath (DAIHAN, CL-30)	0.1 °C	0.0004
Data acquisition system (YOKOGAWA, GP10)	0.01%	0.0001
Flow meter (Dwyer, RMA - 2)	0.5 cc	0.04

with a constant room temperature, and the heat pipe system was shielded by ceramic wool to diminish thermal losses associated with thermal contact. Fig. 5 shows the experimental setup used in this study. As shown in Fig. 5, the bypass line was tightly insulated; thus, thermal contact between the bypass tube and the external environment was prevented. However, the input heat energy may be conducted through the wall of the bypass tube attached to the start of the evaporator. Additionally, the bypass tube located in the condenser may have some cooling due to heat conduction. The heat pipe was installed on a tilt-adjustable workbench to identify the thermal response to the gravitational effect based on orientation.

3. Results and discussion

The coolant temperature was kept constant at 3 °C throughout the entire experiment. The orientation of the heat pipe and the input heat load were specified as experimental variables. The orientation of the heat pipe (φ) was adjusted up to 50° by considering the cooling capacity of the isothermal bath. Before the experiment was conducted to measure the acceleration of the flow of working fluid inside the heat pipe by liquid bypass, preliminary experiments were conducted to confirm the reliability of the experimental device. The test results of these preliminary experiments were reported through references [31,32]. The filling ratio of the operating fluid affects the thermal capacity of the heat pipe. The rise in thermal resistance caused by the liquid pool generated by excessive charging inevitably degrades the heat transfer capacity of a heat pipe. Furthermore, an excessive shortage of working fluid may decrease the thermal load excessively, causing dryout. Usually, the optimal fill charge ratio can be determined experimentally. The optimal charging amounts for a typical heat pipe, as shown in Fig. 3(a). A heat pipe that operates in the *NM* can differ because of the attached bypass ports. In this experiment, the fill charge ratio of the working fluid was experimentally determined for heat pipe operating under *NM*. The difference in heat transfer performance between the typical heat pipe and the heat pipe with *NM* on the basis of the

experimentally obtained favorable charge amount was obtained experimentally, and then the experimental results were provided in the literature [32]. The fill charge ratio of the working fluid, $\Phi = 100\%$, corresponds to the void volume of the groove shown in Fig. 4. As presented in literature [32], the favorable fill charge ratio of the working fluid applied in all experiments was measured to be 120%, and the volume of working fluid filled in the heat pipe was 17.6 ml. As shown in Fig. 3, the heat pipe operating in the *NM* was identical to a typical heat pipe except for the four liquid bypass ports considered in the current study. In preliminary experiments, the thermal resistance between typical and *NM* heat pipes was compared under horizontal inclination and obtained from the literature [31]. In this study, the thermal resistance was used as an index of heat transfer performance, evaluated by Eq. (2).

$$R_{th} = \left(\overline{T}_{evap.} - \overline{T}_{cond.}\right) / Q_{in} \tag{2}$$

expressed as the average outer wall temperature of the evaporator and condenser, which are $\overline{T}_{evap}$ and $\overline{T}_{cond}$, respectively.

An experiment on thermal performance comparison between a typical heat pipe and a heat pipe with a bypass line under *NM* was performed horizontally, and the results were provided in literature [31]. As mentioned [31], the thermal resistance for typical heat pipes was estimated to be lower under relatively low heat loads (50 W and 100 W). However, as the heat load increases, the thermal resistance for the heat pipe with the bypass line under *NM* becomes lower than that of the typical heat pipe. The discrepancy in thermal resistance between the two heat pipes was evaluated as somewhat high at 15.7% at an input thermal load of 50 W; however, this decreased with an increase in the input heat load. Except for the input heat load of 50 W, the mismatch was generally evaluated to be less than 5%; therefore, the heat transfer performance between the typical heat pipe and the heat pipe operating under *NM* was found to be almost equivalent. The uncertainty about thermal resistance presented in Eq. (2) was evaluated by Eq. (3) [34] and provided in the literature [31]. As presented [31], the uncertainty was generally found to be less than 10%.

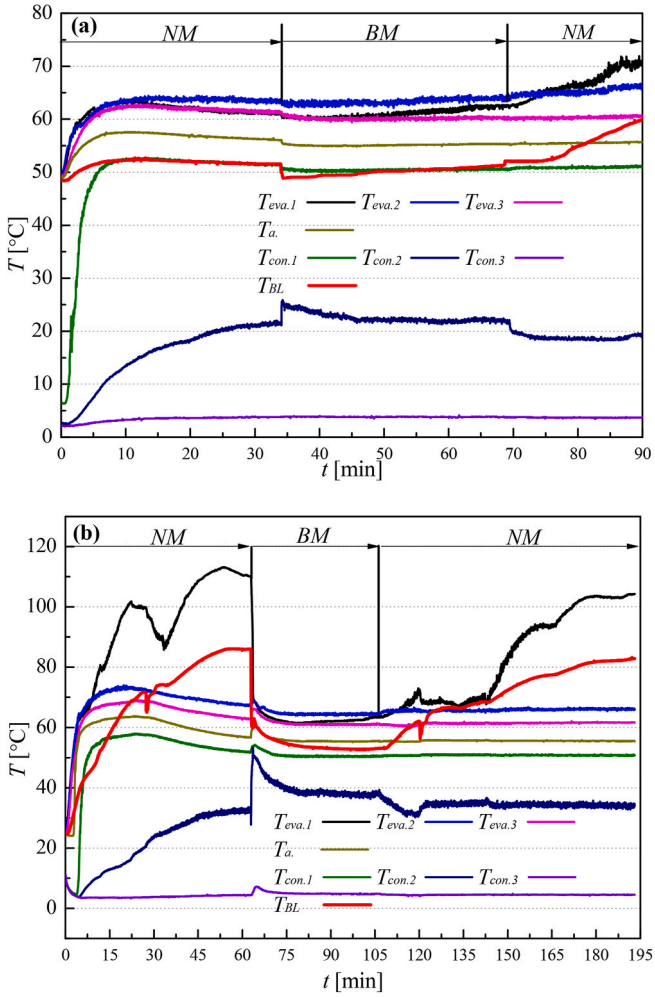

Fig. 6. Start-up and steady-state characteristics of the heat pipe in the *BM* and *NM* for $\varphi = 0$ orientation, based on (a) $Q_{in} = 200$ W, and (b) $Q_{in} = 300$ W.

$$U_{R_{th}} = \pm \left[\left(\frac{\overline{T}_{eva.}}{\overline{T}_{eva.} - \overline{T}_{con.}} \times U_{\overline{T}_{eva.}} \right)^2 + \left(\frac{\overline{T}_{con.}}{\overline{T}_{eva.}} \times U_{\overline{T}_{con.}} \right)^2 + U_{Q_{in}} \right]^{1/2} \quad (3)$$

The recovered heat (Q_{out}) discharged from the condenser to the coolant was considered by Eq. (4).

$$Q_{out} = (\rho \dot{V} c)_{cool} (T_{cool.out} - T_{cool.in}) \quad (4)$$

As shown in Eq. (4), the recovery heat includes the coolant inlet temperature ($T_{cool.in}$), outlet temperature ($T_{cool.out}$), and volumetric rate ($\dot{V}$) of the coolant in the condenser. As shown in Eq. (4), the recovered heat includes the inlet ($T_{cool.in}$) and outlet ($T_{cool.out}$) temperatures of the cooling source and the volumetric flow rate ($\dot{V}$) of the coolant flowing over the condenser surface. In the literature [31], results on the energy balance between input thermal load and recovery heat under horizontal position were provided. The discrepancy between input heat load and recovery heat was generally estimated to be less than 8%.

The objective of this experimental work is to experimentally investigate the acceleration of the working fluid during *BM* operation. The acceleration of the operating fluid was confirmed in accordance with the temperature distribution in the condenser wall. In particular, the temperatures at the center or end of the condenser are useful for comparing the operating-fluid flow. A rise in the temperature of the condenser could indicate that more vapor was transported to the section and that the working fluid can be evaluated as being relatively accelerated. In all experimental processes, the method of opening all bypass values after reaching steady state was used to confirm the acceleration of the operating fluid. The acceleration of the operating fluid by using the bypass tube was examined based on the change in temperature distribution in the condenser before and after opening the valves.

A series of experiments were conducted to observe the acceleration of the working fluid under bypass line operation. In this study, an experimental method was applied so that the acceleration of the working fluid could be easily confirmed by the temperature change of the condenser wall. In other words, temperature changes were observed at the location of interest of the heat pipe due to activation

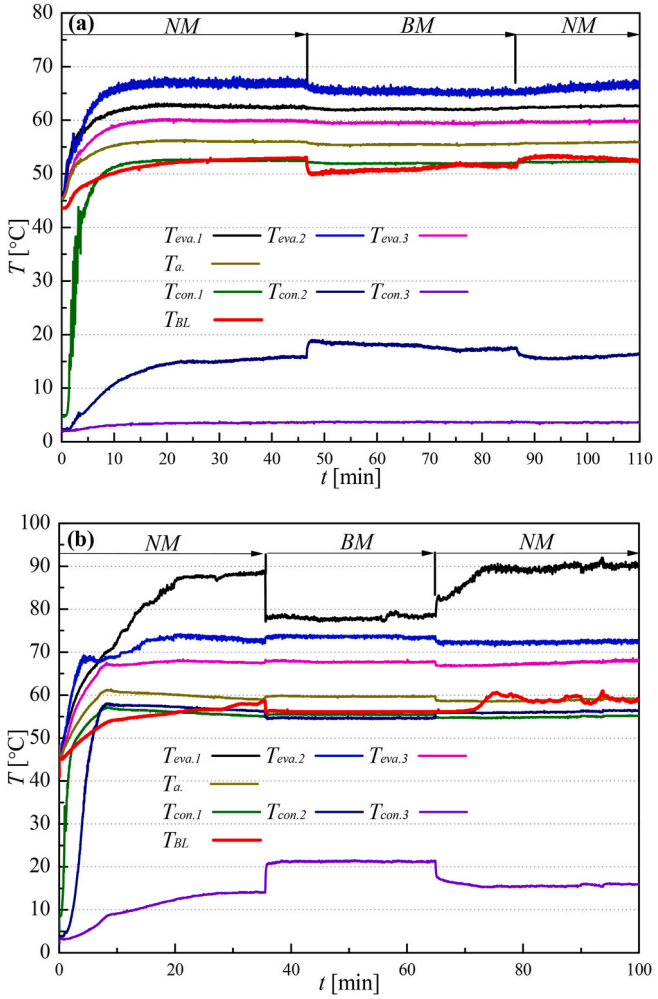

Fig. 7. Start-up and steady-state characteristics of the heat pipe in the *BM* and *NM* for $\varphi = 10$ orientation, based on (a) $Q_{in} = 200$ W, and (b) $Q_{in} = 500$ W.

and deactivation of the bypass line by manual operation of the bypass valves under a constant input heat load. In particular, acceleration of the working fluid was explained by temperature changes obtained in thermocouples attached to the condenser wall according to activation and deactivation of the bypass line.

Figs. 6–11 present the experimental data for the outer wall temperatures of the heat pipe system, which started under the *NM* and switched to the *BM* after achieving a steady state in the horizontal and 10°, 20°, 30°, 40°, and 50° orientations. When the *NM* was switched to *BM*, the working fluid acceleration was identified by comparing the temperature distributions in the condenser. As depicted in Fig. 5, the condensed and cooled liquid in the condenser was bypassed through the bypass line to the beginning of the evaporator. Therefore, the temperature measured by the thermocouple fixed onto the external wall of the bypass tube at the beginning of the evaporator (T_{BL1} in Fig. 5) can be designated as a representative temperature for detecting liquid circulation inside the bypass tube. T_{BL} shown in Figs. 6–11 is defined as T_{BL1} in Fig. 5, which is shown in bold red. T_{BL} decreased under the *BM* operation, wherein the liquid produced by condensation and cooling was bypassed via the bypass line. In addition, since the acceleration of the working fluid can be depicted based on the temperatures obtained from the three thermocouples installed in the condenser, these temperatures are emphasized by a bold blue trend line.

Fig. 6 presents experimental data for the horizontal orientation of heat pipe operation, which began in the *NM* and was switched to the *BM* after attaining a steady state at Q_{in} of 200 W (Fig. 6(a)) and 300 W (Fig. 6(b)). Fig. 6(a) shows that the heat pipe operation started in the *NM*, switched to the *BM* after 34 min on reaching a steady state, and finally returned to the *NM* at 70 min. When the operation of the heat pipe was switched to the *BM*, the difference in the temperatures at the condenser end ($T_{con.3}$) under the *NM* and *BM* was insignificant; however, the temperature in the middle of the section ($T_{con.2}$) increased from 21.5 to 22.4 °C. After switching to *BM*, it was estimated that the temperature of the condenser increased owing to the increment in the vapor-mass flow rate that reached the section. In addition, the average evaporator outer wall temperatures in the *BM* and *NM* were similar (approximately 62.1 °C), but the operating temperature ($T_{a.}$) decreased by approximately 1.4 °C when the *BM* was used. At the end of the experimental period of 70 min, when the operation of the heat pipe returned to the *NM*, the evaporator outer wall temperature ($T_{evap.1}$) increased to 70 °C. The

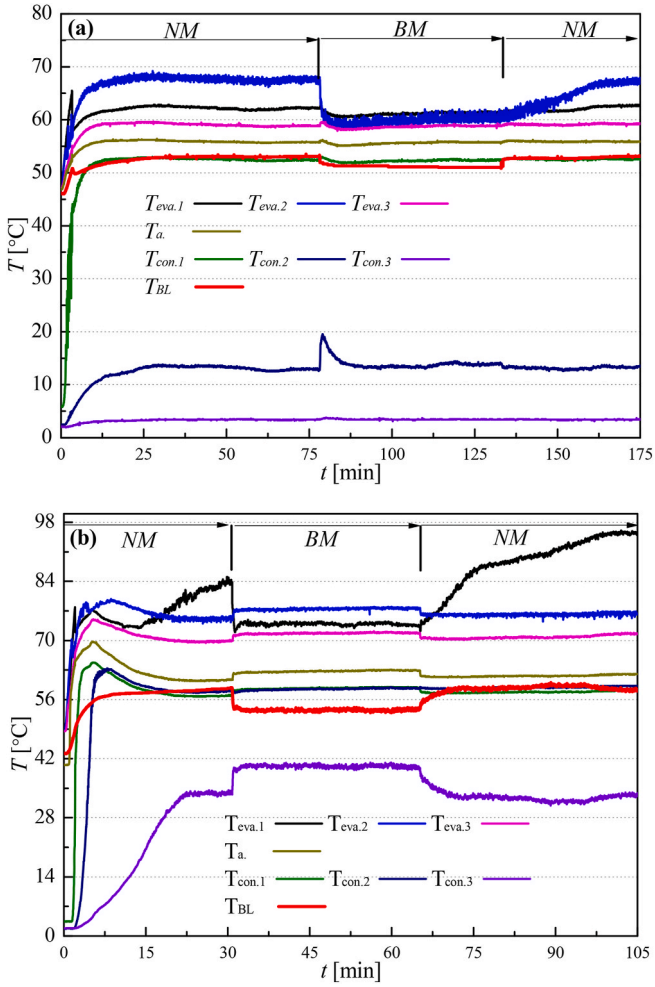

Fig. 8. Start-up and steady-state characteristics of the heat pipe in the *BM* and *NM* for $\varphi = 20$ orientation, based on (a) $Q_{in} = 200$ W, and (b) $Q_{in} = 600$ W.

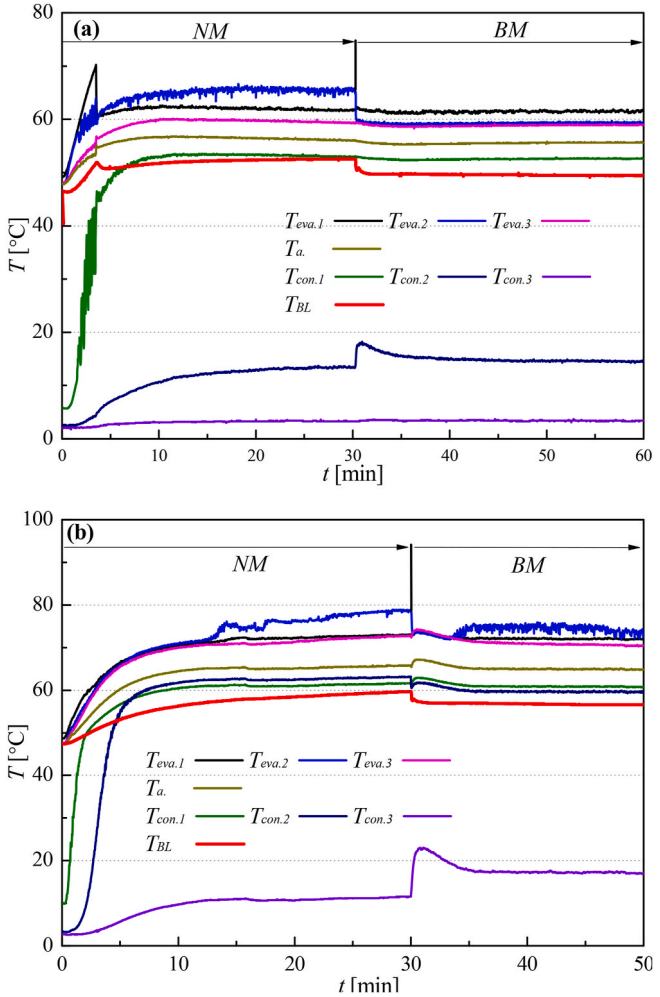

Fig. 9. Start-up and steady-state characteristics of the heat pipe in the *BM* and *NM* for $\varphi = 30$ orientation, based on (a) $Q_{in} = 200$ W, and (b) $Q_{in} = 500$ W.

temperature in the middle of the condenser ($T_{con.2}$) decreased to 18.1 °C. In addition, T_{BL} decreased from 21.9 to 18.3 °C because of the heat inflow from the evaporator, indicating that the volumetric flow rate of vapor to the condenser reduced. When the operation of the heat pipe returned to the *NM*, the temperature of the outer wall of evaporator increased relatively, potentially due to alterations in the flow behavior inside the heat pipe.

Fig. 6(b) presents the results for the heat pipe, which started with *NM*, switched to *BM* at 63 min, and returned to *NM* at 106 min with a Q_{in} of 300 W. As depicted in the figure, the outer wall temperature (T_{BL}) of bypass line decreased from 86.2 to 53 °C because of the inflow of the cooled liquid caused by the switch to the *BM*, indicating liquid circulation in the bypass line. With the switch to the *BM*, the temperature in the middle of the condenser ($T_{con.2}$) increased from 32.6 to 38.2 °C but decreased again to 33.7 °C with the return to the *NM*. When the heat pipe operation was switched to the *BM*, the temperature ($T_{con.3}$) detected by the thermocouple attached at the end of the condenser increased from 4.3 to 4.8 °C. The external wall temperatures of the condenser increased with the switch to *BM* because the vapor-mass flow rate into the section increased. However, a significant reduction in the wall temperature of the evaporator was viewed because of the bypass of the cooled liquid to the end of the section. With the switch to the *BM*, the temperature at the beginning of the evaporator ($T_{eva.1}$) decreased from 110.5 to 62.5 °C. Applying *BM* decreased the evaporator outer wall temperature to 48 °C. The temperature ($T_{eva.2}$) in the middle of the evaporator outer wall decreased from 67.4 to 64.7 °C because of the *BM*. As shown in Fig. 6, the acceleration of the working fluid by liquid bypass was measured with an increase of 5.6 °C and 0.5 °C in the middle and end temperatures ($T_{con.2}$ and $T_{con.3}$) of the condenser outer wall, respectively, under *BM* application at a horizontal position and an input thermal load of 300 W.

Fig. 7 presents the test results of the heat pipe operation that began in the *NM* and switched to the *BM* after achieving a steady state under Q_{in} of 200 and 500 W at $\varphi = 10°$. When Q_{in} was 200 W (Fig. 7(a)), the heat pipe operation started under *NM* and switched to *BM* at 46.2 min, returning to *NM* again at 86.5 min. With the switch to the *BM*, the temperature in the middle of the condenser ($T_{con.2}$) increased from 15.8 to 17.4 °C. The temperature ($T_{con.3}$) measured at the condenser end was approximately 3.6 °C, similar to that under the *NM*. Applying *BM* decreased the external wall temperature of the evaporator. When the heat pipe operation was switched to the

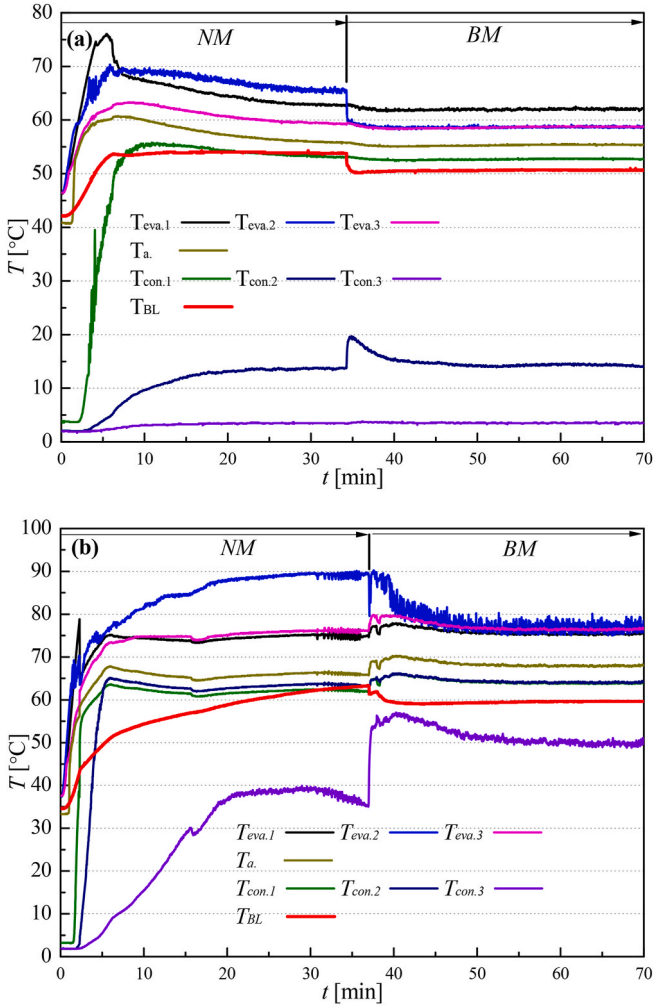

Fig. 10. Start-up and steady-state characteristics of the heat pipe in the *BM* and *NM* for $\varphi = 40$ orientation, based on (a) $Q_{in} = 200$ W, and (b) $Q_{in} = 700$ W.

BM, the wall temperature ($T_{eva.2}$) in the middle of the evaporator decreased from 67.1 to 65.2 °C, and the temperature at the beginning of the section ($T_{eva.1}$) decreased from 62.4 to 62.1 °C. The operating temperature (T_a) decreased marginally from 55.9 to 55.2 °C. As presented in Fig. 7(b), the Q_{in} increased to 500 W. The heat pipe operation was switched to *BM* at an experimental time of 35 min and returned to the *NM* after approximately 65 min. After the switch to the *BM*, the wall temperature (T_{BL}) of the bypass liquid tube decreased from 58.8 to 56.1 °C because of the bypass of the liquid condensed and cooled by the coolant to the beginning of the evaporator. As depicted in Fig. 7(b), a significant acceleration of the working fluid was observed with the application of *BM*. With the switch to the *BM*, the temperature ($T_{con.3}$) measured at the condenser end increased from 14 to 21.3 °C, and the temperature in the middle of the section ($T_{con.2}$) from 54.8 to 55.6 °C. In addition, as the cooled liquid bypassed the beginning of the evaporator, the temperature in this area ($T_{eva.1}$) significantly decreased. With the switch to the *BM*, $T_{eva.1}$ decreased from 88.8 to 77.7 °C. In addition, the temperature ($T_{eva.2}$) measured at the evaporator middle location decreased from 72.5 to 73.8 °C. In contrast, the temperature ($T_{eva.1}$) measured at the evaporator starts increased by approximately 1 °C. As shown in Fig. 7, under a tilt angle of 10° and an input thermal load of 500, the mid and end temperatures ($T_{con.2}$ and $T_{con.3}$) of the condenser were found to increase by 0.8 °C and 7.3 °C due to the application of *BM*, respectively. Therefore, significant acceleration of the working fluid was observed due to the application of liquid bypass.

Fig. 8 presents the experimental achievements of the heat pipe operation that began in the *NM* and switched to the *BM* after achieving a steady state under Q_{in} of 200 W (Fig. 8(a)) and 600 W (Fig. 8(b)) at $\varphi = 20°$. Fig. 8(a) depicts the experimental results pertaining to the heat pipe, which started under *NM*, switched to *BM* at 78 min, and returned to *NM* again at 133.5 min under a Q_{in} of 200 W and $\varphi = 20°$. With the switch to the *BM*, the bypass outer wall temperature (T_{BL}) decreased from 52.9 to 52.4 °C. As shown in Fig. 8(a), with the switch to the *BM* operation, the temperature ($T_{con.3}$) measured at the condenser end remained similar, but the temperature in the middle of the section ($T_{con.2}$) increased from 12.9 to 14.1 °C. With the application of the *BM*, the temperature at the beginning of the evaporator ($T_{eva.1}$) decreased from 62.4 to 62.1 °C because of the bypass of the cooled liquid. In particular, the temperature in the middle of the section ($T_{eva.2}$) decreased from 67.9 to 60.2 °C. When the heat pipe operation returned to *NM*, the

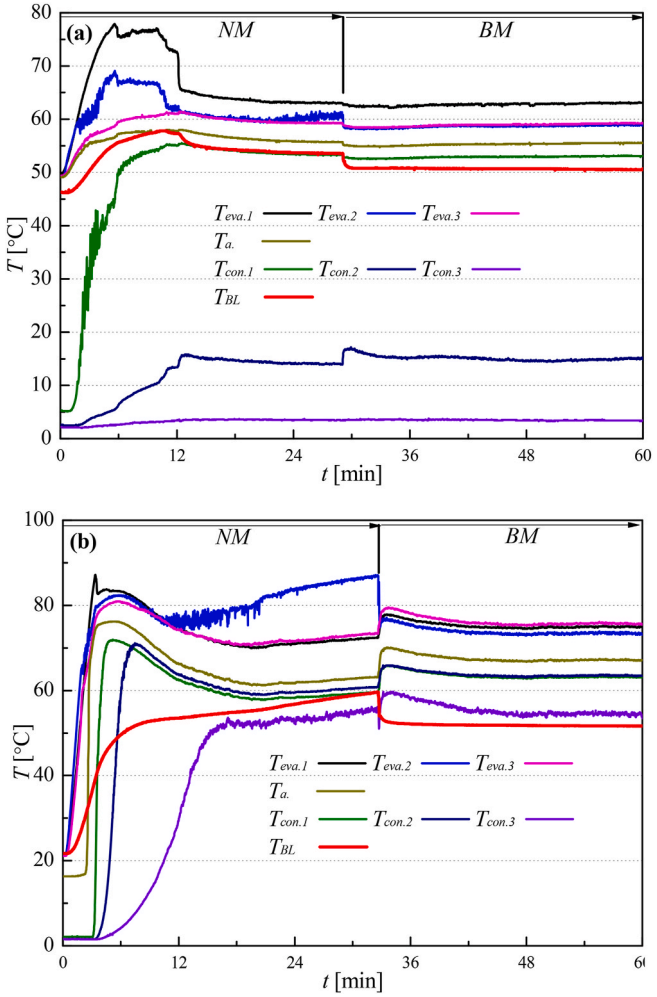

Fig. 11. Start-up and steady-state characteristics of the heat pipe in the *BM* and *NM* for $\varphi = 50$ orientation, based on (a) $Q_{in} = 200$ W, and (b) $Q_{in} = 700$ W.

outer wall temperatures ($T_{eva.1}$ and $T_{eva.2}$) measured at the evaporator wall increased, whereas the temperature ($T_{con.3}$) measured at the condenser end decreased again. As depicted in Fig. 8(b), the acceleration of the operating fluid is higher under a Q_{in} of 600 W. As observed from the figure, the temperature ($T_{con.3}$) measured at the condenser end increased from 33.8 to 40.3 °C as a result of the application of the *BM* at 30.7 min. In addition, with the *BM* application, $T_{con.1}$ increased from 57 to 58.9 °C. When the heat pipe operation was returned to the *NM* again at 65 min, $T_{con.3}$ decreased to 33.3 °C. In addition, $T_{eva.1}$ increased from 73.9 to 95.4 °C. As shown in Fig. 8, under the conditions of a tilt angle of 20° and an input thermal load of 600 W, the temperature at the start ($T_{con.1}$) and end ($T_{con.3}$) of the condenser due to liquid bypass increased by 1.9 °C and 6.5 °C, respectively. Considering the increase in condenser wall temperatures due to the application of *BM*, the vapor velocity can be evaluated to be significantly increased compared to that of the heat pipe with *NM*.

Fig. 9 provides the test results for the heat pipe operation that started under *NM* and switched to *BM* after reaching a steady state under a Q_{in} of 200 W (Fig. 9(a)) and 500 W (Fig. 9(b)) at $\varphi = 30°$. At an Q_{in} of 200 W, T_{BL} reduced from 52.6 to 52.2 °C with the switch to the *BM*. Under a low Q_{in} of 200 W, *NM* and *BM* exhibited similar $T_{con.3}$ values. However, $T_{con.2}$ increased from 13.4 to 14.7 °C with the switch to the *BM*, indicating the acceleration of the working fluid. Switching to *BM* decreases the temperature measured on the evaporator out wall. $T_{eva.2}$ significantly decreased from 65.6 to 59.4 °C, and $T_{eva.3}$ decreased from 59.4 to 58.9 °C. As depicted in Fig. 9 (b), when the BM operation was applied for 30 min under a Q_{in} of 500 W, the temperature ($T_{con.3}$) measured at the condenser end increased significantly, indicating the acceleration of the working fluid. With the switch to the *BM*, $T_{con.3}$ increased from 11.5 to 17.3 °C. The application of *BM* decreased the temperature measured at the evaporator outer wall. $T_{eva.2}$ decreased from 78.8 to 73.1 °C, and $T_{eva.1}$ from 73 to 72.1 °C. $T_{eva.3}$ decreased from 72.8 to 70.3 °C. As mentioned in Fig. 13, at $\varphi = 30°$ and an input thermal load of 200 W, the middle temperature ($T_{con.2}$) of the condenser wall increased by 1.3 °C, and under an input thermal load of 500 W, the temperature ($T_{con.3}$) at the end of the condenser wall increased by 5.8 °C. From these results, it could be estimated that the vapor inside the heat pipe travels faster under *BM*.

Fig. 10 illustrates the test results for the heat pipe operation that started under *NM* and switched to *BM* after reaching a steady state

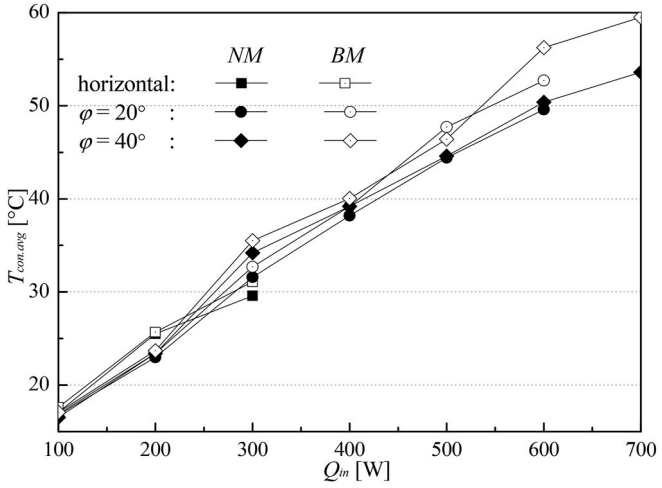

Fig. 12. Comparison of the average outer wall temperature of the condenser between *NM* and *BM* according to the Q_{in} under $\varphi = 0°$, 20° and 40°.

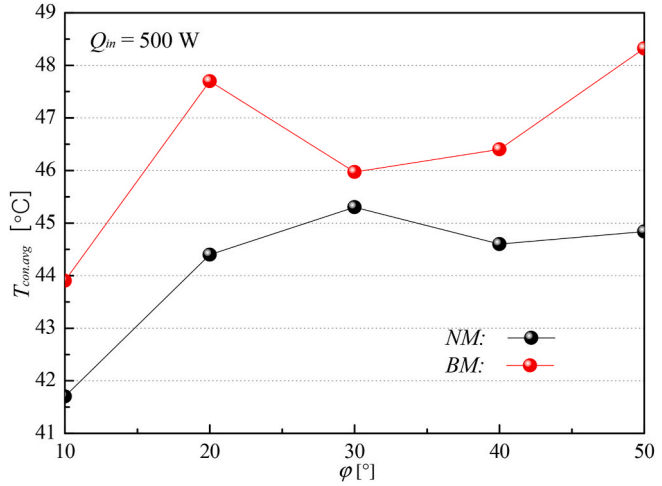

Fig. 13. Comparison of the average outer wall temperature of the condenser between *NM* and *BM* according to the φ under $Q_{in} = 500$ W.

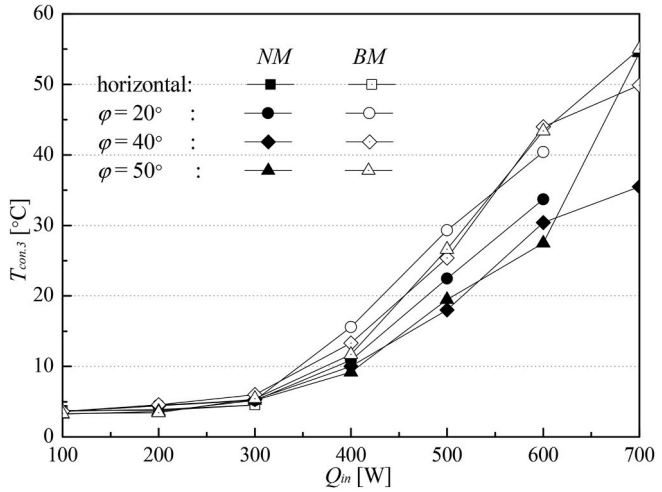

Fig. 14. Comparison of the $T_{con.3}$ between *NM* and *BM* according to the Q_{in} under $\varphi = 0°$, 20°, 40° and 50°.

under Q_{in} of 200 W (Fig. 10(a)) and 700 W (Fig. 10(b)) at $\varphi = 40°$. As shown in Fig. 10(a), when the heat pipe operation was switched to the *BM* at approximately 34.3 min, liquid circulation in the bypass tube was measured as T_{BL} decreased from 53.8 to 52.2 °C. At a low Q_{in} of 200 W, the differences in the $T_{con.3}$ values for the *NM* and *BM* were insignificant. However, $T_{con.2}$ increased by approximately 0.7 °C under the *BM* compared to that under the *NM*, thereby showing the acceleration of the working fluid. The application of *BM* decreased the temperature measured at the evaporator outer wall. As exhibited in Fig. 10(a), $T_{eva.2}$ decreased from 65.7 to 58.7 °C, and $T_{eva.1}$ decreased from 62.8 to 61.9 °C. $T_{eva.3}$ decreased from 59.4 to 58.9 °C. However, significant acceleration of the working fluid was observed under a high Q_{in} of 700 W. As indicated in Fig. 10(b), heat pipe operation was switched to *BM* at 37.2 min. With the switch to the *BM*, $T_{con.3}$ increased from 35 to 50.1 °C, confirming that a higher mass flow rate of vapor reached the condenser end, indicating the acceleration of the working fluid. $T_{con.2}$ increased from 63.5 to 64.1 °C, and $T_{con.1}$ increased from 61.9 to 63.9 °C. A reduction in temperature measured at the evaporator outer wall was viewed because of the bypass of the liquid cooled in the condenser. $T_{eva.2}$ decreased from 89.7 to 77.1 °C. $T_{eva.1}$ and $T_{eva.3}$ were slightly increased by the *BM* operation, but the increment was measured to be under 0.4 °C. As shown in Fig. 14, under $\varphi = 40°$ and an input thermal load of 700 W, the steady-state temperatures at the start ($T_{con.1}$), middle ($T_{con.2}$), and end ($T_{con.3}$) of the condenser wall increased by 2 °C, 0.6 °C, and 15.1 °C, respectively. From these test results, it can be assumed that there was a significant increase in vapor flow by applying *BM*.

Fig. 11 depicts the experimental findings wherein the heat pipe was started under the *NM* and switched to the *BM* after reaching a steady state under the Q_{in} of 200 W (Fig. 11(a)) and 700 W (Fig. 11(b)) at $\varphi = 50°$. As illustrated in Fig. 11(a), when a relatively low Q_{in} of 200 W was applied, $T_{con.3}$ was measured to be approximately 3.7 °C for both the *NM* and *BM*, indicating that it was not affected by the operation mode. However, $T_{con.2}$ increased from 14.1 to 15.3 °C because of the *BM* operation, showing the acceleration of the operating fluid. In the case of the temperatures in the evaporator outer wall, $T_{eva.2}$ decreased from 60.9 to 58.9 °C because of the application of the *BM*. The temperatures in the evaporator outer wall were similar in both operation modes. When the *BM* was applied at 32.5 min under a high Q_{in} of 700 W, $T_{con.2}$ increased from 60.9 to 63.7 °C owing to the acceleration of the working fluid, and $T_{con.3}$ was measured to be similar. $T_{con.1}$ increased from 59.8 to 63 °C. The mean temperature for the evaporator outer wall decreased by 2.8 °C because of the bypass of the liquid in the condenser. As shown in Fig. 15, a grater acceleration effect by applying *BM* was measured with an increase in input thermal load. Under an input thermal load of 200 W, the wall temperature in the middle of the condenser increased by 1.2 °C, but under that of 700 W, it increased by 2.8 °C.

As shown in Figs. 6–11, the condenser wall temperature usually increased when the operation of the heat pipe was switched from *NM* to *BM*. By reducing the liquid flow rate inside the heat pipe via the bypass tube during the *BM* operation, it was possible to alleviate the flow resistance over the phase change interface between the vapor and liquid with counter flow. This could cause a higher vapor flow rate to reach the condenser by accelerating the working fluid. Based on this factor, the condenser wall temperature typically increases. Moreover, the temperatures in the evaporator outer wall were reduced as a result of the bypass of the liquid that had been cooled in the condenser to the evaporator via the bypass line. Therefore, the liquid bypass by the bypass tube reduced the temperature variance between the evaporator and condenser by decreasing the evaporator outer wall temperature and increasing the condenser outer wall temperature. Thus, the R_{th} of heat pipe (Eq. (2)) can be significantly reduced. Figs. 12–17 compare the steady-state heat transfer performance between heat pipes with *BM* and *NM*. As explained in Figs. 6–11, the heat transfer performance of the heat pipe was significantly improved by applying *BM* because the condenser wall temperatures generally increased, while the evaporator wall temperatures decreased due to liquid bypass.

Fig. 12 shows the mean outer-surface temperature of the condenser in accordance with input thermal load at $\varphi = 0°$, 20°, and 40°. As presented in Fig. 12, the mean temperature was typically higher under the *BM* operation than under the *NM* operation. The average temperature difference increased with the Q_{in}. At $\varphi = 0°$, the mean temperatures of the two running modes were estimated to be similar at $Q_{in} = 100$ W. However, when Q_{in} was increased to 300 W, the average temperature in the *BM* was investigated to be 1.5 °C higher in comparison to that in the *NM*. In the case of $\varphi = 20°$, the average temperature under the *BM* was measured to be 3.3 °C higher in

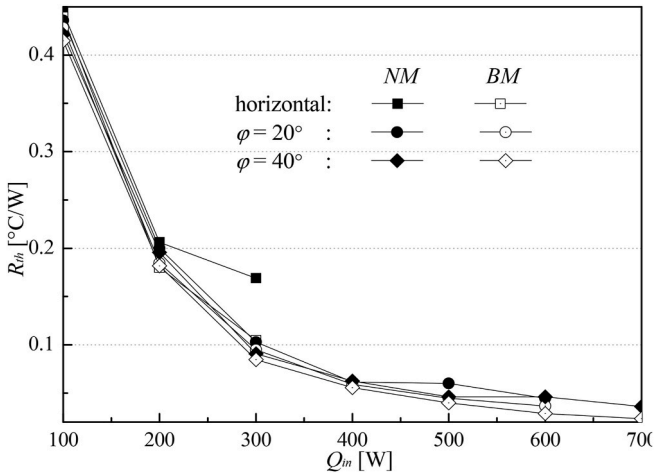

Fig. 15. Comparison of the R_{th} between *NM* and *BM* according to the Q_{in} under $\varphi = 0°$, 20° and 40°.

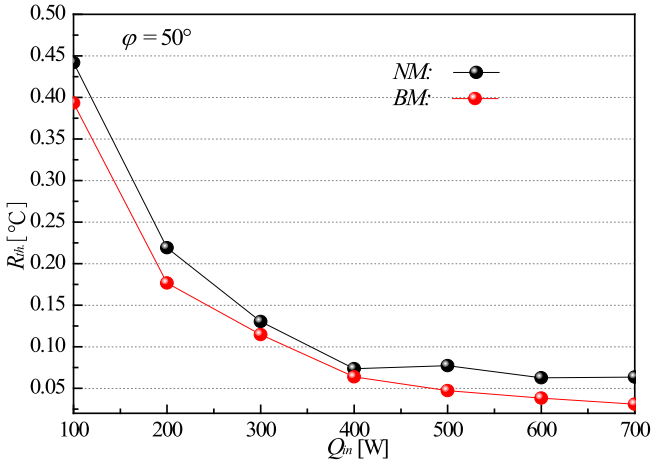

Fig. 16. Comparison of the R_{th} between *NM* and *BM* according to the Q_{in} under $\varphi = 50°$.

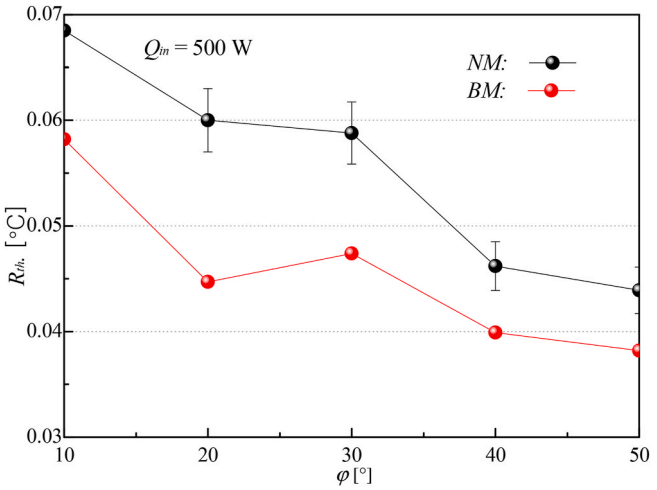

Fig. 17. Comparison of the R_{th} between *NM* and *BM* according to the φ under $Q_{in} = 500$ W.

comparison to that under the *NM* at a Q_{in} of 600 W. Under $\varphi = 40°$ and $Q_{in} = 700$ W, the average temperature under the *BM* operation was estimated to be approximately 6 °C higher in comparison to that under the *NM*.

Fig. 13 compares the mean temperatures of the condenser outer wall in the *NM* and *BM* based on the orientation of the heat pipe at $Q_{in} = 500$ W. As shown in Fig. 13, when the heat pipe is operated in the *BM*, the acceleration of the working fluid is indicated by a high average measured temperature. The average temperature was measured to be 2.2, 3.3, 0.67, 1.8, and 3.48C° higher under the *BM* operation compared to the *NM* at orientations of $\varphi = 10°$, 20°, 30°, 40°, and 50°, respectively.

Fig. 14 compares the $T_{con.3}$ values in the *NM* and *BM* at $\varphi = 0°$, 20°, 40°, and 50°. As shown in the figure, a higher $T_{con.3}$ was measured under *BM* operation than under *NM* operation, and the average temperature difference increased with the Q_{in}. At a relatively low Q_{in} of 300 W or less, low temperatures of 6 °C or less were measured in both operation modes because sufficient vapor could not reach the end of the condenser, and the difference in $T_{con.3}$ between the *BM* and *NM* was insignificant. When the Q_{in} was increased to 400 W or higher, a significant increase in $T_{con.3}$ caused by the application of the *BM* was observed. At $\varphi = 20°$, the average temperature under the *BM* was measured to be 6.8 °C higher than that under the *NM* at an input thermal load of 600 W. Under $\varphi = 40°$ and $Q_{in} = 700$ W, $T_{con.3}$ under the *BM* was measured to be approximately 14.4 °C higher than that under the *NM*. Under $\varphi = 50°$ and $Q_{in} = 600$ W, $T_{con.3}$ under the *BM* was observed to be approximately 15.9 °C higher in comparison to that under the *NM*.

Fig. 15 shows the R_{th} values of the heat pipe based on the input thermal load at $\varphi = 0°$, 20°, and 40°. As explained in Figs. 6–11, the mean temperature of the evaporator outer wall decreased, and the average outer wall temperature of the condenser increased under *BM* operation compared to *NM*. As shown in Eq. (2), R_{th} decreases with the deviation in the mean temperatures of the evaporator and condenser outer walls. Therefore, R_{th} was calculated to be lower under *BM* conditions than under *NM* conditions. As shown in Fig. 15, R_{th} was usually lower under *BM* operation than under *NM* operation, and the R_{th} of *BM* became significantly reduced compared to that of *NM* as the Q_{in} increased. At $\varphi = 0°$, the R_{th} of the *BM* was 1% lower than that of the *NM* at $Q_{in} = 100$ W. However, at $Q_{in} = 300$ W, the

R_{th} of the *BM* was 38% lower than that of the *NM*. At $\varphi = 20°$, the R_{th} of *BM* was calculated to be 25.5% lower than that of *NM* at a Q_{in} of 500 W. For $\varphi = 40°$ and $Q_{in} = 700$ W, the R_{th} of *BM* was calculated to be 37.3% lower than that of *NM*.

Fig. 16 shows the R_{th} of the heat pipe with respect to the Q_{in} at $\varphi = 50°$. As illustrated, R_{th} was lower under *BM* operation than under *NM* operation across the entire thermal load range, and the R_{th} of *BM* significantly reduced as the Q_{in} increased. The R_{th} of the BM was 12.3% lower than that of the *NM* at $Q_{in} = 100$ W; however, it was 106.5% lower at $Q_{in} = 700$ W.

Fig. 17 compares the R_{th} values of the *NM* and *BM* according to the orientation of the heat pipe at $Q_{in} = 500$ W. As shown in Fig. 17, when the heat pipe is operated in the *BM*, the acceleration of the operating fluid is measured by the high average temperature. The average temperature was calculated to be 14 C°, 12 C°, 12.9C°, 37 C°, and 24.4C° lower under the *BM* operation compared to the *NM* at orientations of $\varphi = 10°$, 20°, 30°, 40°, and 50°.

Fig. 18 shows the maximum thermal load (Q_{max} at which the heat pipe can operate normally according to the orientation angle φ in each operating condition. Clearly, the Q_{max} of the heat pipe with *BM* increased compared to that of the heat pipe operating under *NM*. In the case of *BM*, for which all bypass ports in the condenser were activated, Q_{max} increased by 10.3% ($\varphi = 15°$) to 45.8% ($\varphi = 0°$) compared to the values for *NM*. Q_{max} increased the most significantly when the heat pipe had $\varphi = 0°$ because at that angle, the portion of the bypassed flow rate for the entire liquid increased. This change occurred because the liquid remained in the condenser for a longer period of time, compared to the time periods for other φ values. In addition, Q_{max} was measured to be significantly higher for $\varphi = 50°$ than for the other φ values (exceeding 0°). No experiment was performed for $\varphi > 50°$ because of the limited capacity of the isothermal bath. Additional experiments at higher φ should be conducted in the future.

4. Conclusions

A set of experiments were conducted to examine the acceleration performance of the working fluid utilizing liquid bypass. For liquid bypass, a bypass tube was connected from the condenser to the beginning of the evaporator. Three liquid ports were attached to the condenser to increase the liquid bypass mass-flow rate. In all the experiments, the heat pipe operation started in the *NM* (with all bypass valves closed) and switched to the *BM* (with all bypass valves opened) after attaining a steady state. The following conclusions were drawn from the experiments:

(1) The temperature of the condenser outer wall increased with the switch from *NM* to *BM*, indicating that a higher mass flow rate of vapor reached the condenser under *BM* operation. Because of this, it could be estimated that the vapor inside the heat pipe moves to the condenser more quickly than that in the heat pipe operated at *NM*.
(2) As the Q_{in} increased, the working fluid acceleration performance of the *BM* operation improved. Under *BM* operation, as the Q_{in} increased, the temperature measured using the thermocouple attached to the end of the condenser reached up to 15.9 °C ($\varphi = 50°$ and $Q_{in} = 600$ W).
(3) Applying the *BM* significantly decreased the temperature of the evaporator outer wall because of the bypass of the liquid condensed and cooled in the condenser to the beginning of the evaporator. For example, under $\varphi = 50°$ and $Q_{in} = 600$ W, the temperature at the beginning of the evaporator decreased by 48 °C from 110.5 to 62.5 °C because of the application of the BM.
(4) Applying the *BM* reduced the temperature difference between the evaporator and condenser by decreasing the average evaporator outer wall temperature and increasing the mean temperature in condenser outer wall, which decreased the R_{th} of the heat pipe by up to 38% ($\varphi = 0°$ and $Q_{in} = 300$).
(5) When *BM* was applied at $\varphi = 0°$ and 50°, the maximum thermal load increased to 45.8% and 25.3%, respectively.

As mentioned in (1)–(4) above, applying the *BM* can improve the acceleration performance of the operating fluid by fundamentally alleviating the flow resistance over the phase-change interface that occurs inside a heat pipe. Significant research is needed on the design of the auxiliary loop to enable more condensate to be diverted from the condenser to the evaporator via an effective liquid

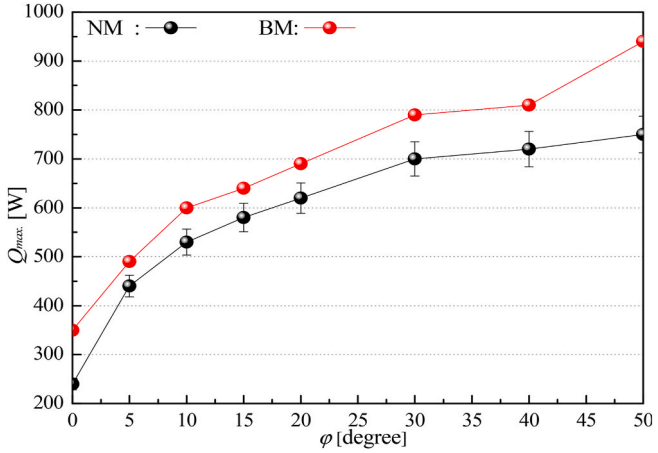

Fig. 18. Q_{max} of the heat pipe under *NM* and *BM* conditions versus φ

bypass technology.

Credit author statement

Cheong Hoon Kwon: Conceptualization, Methodology/Study design, Validation, Investigation, Resources, Data curation, Writing – review and editing, Funding acquisition. Hyuk Su Kwon: Methodology/Study design, Data curation. Hyun Ung Oh: Methodology/Study design, Investigation, Writing – original draft, Writing – review and editing, Supervision. Eui Guk Jung: Conceptualization, Methodology/Study design, Formal analysis, Investigation, Writing – original draft, Writing – review and editing, Supervision, Project administration, Funding acquisition.

Declaration of competing interest

The authors declare that they have no known competing financial interests or personal relationships that could have appeared to influence the work reported in this paper.

Data availability

No data was used for the research described in the article.

Acknowledgements

This study was supported by a National Research Foundation (NRF) grant funded by the Ministry of Science (Nos. 2022R1F1A1066459 and NRF-2022R1A2C1009690). This research was supported by a university innovation support project through the National Research Foundation of South Korea funded by the Ministry of Education.

References

[1] R.S. Gaugler, Heat transfer device, 1944. U.S. Patent 2, 350, 348.
[2] G.M. Grover, Evaporation-condensation heat transfer device, 1966. U.S. Patent 3,229,759.
[3] G.P. Peterson, An Introduction to Heat Pipes: Modeling, Testing, and Applications, John Wiley & Sons, New York, NY, USA, 1994.
[4] Z. Zhao, G. Peng, Y. Zhang, D. Zhang, Heat transfer performance of flat micro-heat pipe with sintered multi-size copper powder wick, Case Stud. Therm. Eng. 42 (2023), 102720.
[5] J. Zhao, Y. Ji, D.Z. Yuan, Y.X. Guo, S.W. Zhou, Structural effect of internal composite wick on the anti-gravity heat transfer performance of a concentric annular high-temperature heat pipe, Int. Commun. Heat Mass Tran. 139 (2022), 106404.
[6] F.H.S. Ginting, A.P. Tetuko, N.S. Asri, L.F. Nurdiyansah, E.A. Setiadi, S. Humaidi, Surface treatment on metal foam wick of a ferrofluid heat pipe, Surface. Interfac. 36 (2023), 02499.
[7] X. Jiang, H. Tang, Y. Liu, L. Lian, The heat transfer capacity of multi-layer wick heat pipe tested in anti-gravity orientations, Appl. Therm. Eng. 200 (2022), 117611.
[8] S.C. Wong, W.S. Liao, Visualization experiments on flat-plate heat pipes with composite mesh-groove wick at different tilt angles, Int. J. Heat Mass Tran. 123 (2018) 839–847.
[9] Z. Cui, L. Jia, Z. Wang, C. Dang, L. Yin, Thermal performance of an ultra-thin flat heat pipe with striped super-hydrophilic wick structure, Appl. Therm. Eng. 208 (2022), 118249.
[10] S. Huang, Z. Wan, X. Zhang, X. Yang, Y. Tang, Evaluation of capillary performance of a stainless steel fiber–powder composite wick for stainless steel heat pipe, Appl. Therm. Eng. 148 (2019) 1224–1232.
[11] S.M. Henein, A.A. Abdel-Rehim, The performance response of a heat pipe evacuated tube solar collector using MgO/MWCNT hybrid nanofluid as a working fluid, Case Stud. Therm. Eng. 33 (2022), 101957.
[12] B. Zhang, Z. He, W. Wang, J. Wang, H. Mikulčić, J.J. Klemeš, Investigation on the thermal performance of flat-plate heat pipes with various working fluids under different inclination angles, Energy Rep. (2022) 8017–8026.
[13] D.Y. Aydın, M. Gürü, A. Sözen, E. Çiftçi, Thermal performance improvement of the heat pipe by employing dolomite/ethylene glycol nanofluid, Int. J. Renew. Energy Dev. 9 (2020) 23–27.
[14] D.Y. Aydın, E. Çiftçi, M. Gürü, A. Sözen, The impacts of nanoparticle concentration and surfactant type on thermal performance of a thermosyphon heat pipe working with bauxite nanofluid, Energy Sources, Part A Recovery, Util. Environ. Eff. 43 (12) (2021) 1524–1548.
[15] D.Y. Aydin, M. Gürü, A. Sözen, E. Çiftçi, Investigation of the effects of base fluid type of the nanofluid on heat pipe performance, Proc. IMechE Part A: J. Power Energy 235 (1) (2021) 124–138.
[16] E. Çiftçi, M. Gürü, A. Sözen, Enhancement of thermal performance of the air-to-air heat pipe heat exchanger (AAHX) with aluminate spinel-based binary hybrid nanofluids, Heat Tran. Res. 52 (17) (2021) 81–97.
[17] R.A.A. Babat, K. Martin, E. Çiftçi, A. Sözen, Experimental study on the utilization of magnetic nanofluids in an air-to-air heat pipe heat exchanger, Chem. Eng. Commun. 210 (5) (2023) 687–697.
[18] M. Zhang, Z. Liu, G. Ma, S. Cheng, The experimental study on flat plate heat pipe of magnetic working fluid, Exp. Therm. Fluid Sci. 33 (2009) 1100–1105.
[19] A. Jahanbakhsh, H.R. Haghgou, S. Alizadeh, Experimental analysis of a heat pipe operated solar collector using water–ethanol solution as the working fluid, Sol. Energy 118 (2015) 267–275.
[20] A. Faghri, Heat Pipe Science and Technology, first ed., Taylor & Francis, 1995.
[21] Y.F. Maydanik, Loop heat pipes, Appl. Therm. Eng. 25 (2005) 635–657.
[22] Y. Wu, J. Cheng, H. Zhu, H. Xue, Q. Lu, Y. Li, W. Li, H. Tao, Experimental study on heat transfer characteristics of separated heat pipe with compact structure for spent fuel pool, Ann. Nucl. Energy 181 (2023), 109580.
[23] Z. Kang, D. Shou, J. Fan, Numerical study of single-loop pulsating heat pipe with porous wicking layer, Int. J. Therm. Sci. 179 (2022), 107614.
[24] Z. Kang, D. Shou, J. Fan, Numerical study of single-loop pulsating heat pipe with porous wicking layer, Int. J. Therm. Sci. 179 (2022), 107614.
[25] Z. Kang, D. Shou, J. Fan, Numerical study of a novel single-loop pulsating heat pipe with separating walls within the flow channel, Appl. Therm. Eng. 196 (2021), 117246.
[26] V.K. Patel, An efficient optimization and comparative analysis of ammonia and methanol heat pipe for satellite application, Energy Convers. Manag. 165 (2018) 382–395.
[27] P.R. Mashaei, M. Shahryari, Effect of nanofluid on thermal performance of heat pipe with two evaporators: application to satellite equipment cooling, Acta Astronaut. 111 (2015) 345–555.

[28] Y. Li, N. Li, B. Shao, D. Dong, Z. Jiang, Theoretical and experimental investigations on the supercritical startup of a cryogenic axially Ω-shaped grooved heat pipe, Appl. Therm. Eng. 222 (2023), 119951.
[29] E.G. Jung, J.H. Boo, Enhancement of the maximum heat transfer rate of the heat pipe through the bypass line, Appl. Therm. Eng. 198 (2021), 117461.
[30] Y.M. Baek, E.G. Jung, Experimental study on start-up and steady-state heat transfer performance of heat pipe with liquid bypass line for accelerating working fluid, Case Stud. Therm. Eng. 29 (2022), 101708.
[31] C.H. Kwon, G.C. Jin, J.H. Kim, B.G. Im, J.H. Jeong, E.G. Jung, Influence of condenser bypass port area on maximum thermal load of heat pipe, Int. Commun. Heat Mass Tran. 148 (2023), 107006.
[32] C.H. Kwon, H.C. Kwon, E.G. Jung, An experimental investigation on the influence of condenser bypass area for the transient and steady-state heat-transfer performance of heat pipes, Int. Commun. Heat Mass Tran. 148 (2023), 1077057.
[33] The American society of mechanical engineers, Test uncertainty, ASME PTC 19 (1) (2005).
[34] J.P. Holman, Experimental Methods for Engineers, McGraw-Hill, 1996.